



Deposited via The University of York.

White Rose Research Online URL for this paper:

<https://eprints.whiterose.ac.uk/id/eprint/150819/>

Version: Accepted Version

---

**Article:**

Wilkening, S., Schmitt, F. J., Lenz, O. et al. (2019) Discriminating changes in intracellular NADH/NAD<sup>+</sup> levels due to anoxicity and H<sub>2</sub> supply in *R. eutropha* cells using the Frex fluorescence sensor. *Biochimica et Biophysica Acta - Bioenergetics*. 148062. ISSN: 0005-2728

<https://doi.org/10.1016/j.bbabi.2019.148062>

---

**Reuse**

This article is distributed under the terms of the Creative Commons Attribution-NonCommercial-NoDerivs (CC BY-NC-ND) licence. This licence only allows you to download this work and share it with others as long as you credit the authors, but you can't change the article in any way or use it commercially. More information and the full terms of the licence here: <https://creativecommons.org/licenses/>

**Takedown**

If you consider content in White Rose Research Online to be in breach of UK law, please notify us by emailing [eprints@whiterose.ac.uk](mailto:eprints@whiterose.ac.uk) including the URL of the record and the reason for the withdrawal request.

Highlights to

Discriminating changes in intracellular NADH/NAD<sup>+</sup> levels due to anoxicity and H<sub>2</sub> supply in *R. eutropha* cells using the Frex fluorescence sensor

by S. Wilkening, F.-J. Schmitt, O. Lenz, I. Zebger, M. Horch, and T. Friedrich

- The Frex fluorescence sensor reports [NADH] changes in *Ralstonia eutropha*
- The reduced NADH sensitivity of Frex is suitable for NADH monitoring in bacteria
- Frex signals relate to activity of the soluble hydrogenase (SH) upon H<sub>2</sub> supply
- Frex discriminates NADH changes due to anoxicity from SH activity

# Discriminating changes in intracellular NADH/NAD<sup>+</sup> levels due to anoxicity and H<sub>2</sub> supply in *R. eutropha* cells using the Frex fluorescence sensor

Authors: S. Wilkening<sup>1</sup>, F.-J. Schmitt<sup>1</sup>, O. Lenz<sup>1</sup>, I. Zebger<sup>1</sup>, M. Horch<sup>1,2</sup>, and T. Friedrich<sup>1\*</sup>

<sup>1</sup> Technische Universität Berlin, Institut für Chemie PC 14, Straße des 17. Juni 135, 10623 Berlin, Germany

<sup>2</sup> Department of Chemistry and York Biomedical Research Institute, University of York, YO10 5DD, United Kingdom

\* Corresponding author, E-mail: [friedrich@chem.tu-berlin.de](mailto:friedrich@chem.tu-berlin.de)

Keywords:

fluorescence sensor protein; redox sensing; NADH; NAD<sup>+</sup>; Frex; *R. eutropha*; soluble hydrogenase; light-driven bio-hydrogen production

List of abbreviations:

cpFP – circularly permuted fluorescent protein, cpYFP – circularly permuted yellow fluorescent protein, FGN – fructose-glycerol-nitrogen (medium), FN – fructose-nitrogen (medium), Frex – fluorescent Rex, GN – glycerol-nitrogen medium, LB – Luria Bertani (medium), MBH – membrane-bound hydrogenase, NAD – nicotinamide adenine dinucleotide, NAD<sup>+</sup> – oxidized nicotinamide adenine dinucleotide, NADH – reduced nicotinamide adenine dinucleotide, NADP – nicotinamide adenine dinucleotide phosphate, NADPH – reduced nicotinamide adenine dinucleotide phosphate, NADP<sup>+</sup> – oxidized nicotinamide adenine dinucleotide phosphate, OD – optical density, RH – regulatory hydrogenase, SH – soluble NAD<sup>+</sup>-reducing hydrogenase, YFP – yellow fluorescent protein

## Abstract

The hydrogen-oxidizing “Knallgas” bacterium *Ralstonia eutropha* can thrive in aerobic and anaerobic environments and readily switches between heterotrophic and autotrophic metabolism, making it an attractive host for biotechnological applications including the sustainable H<sub>2</sub>-driven production of hydrocarbons. The soluble hydrogenase (SH), one out of four different [NiFe]-hydrogenases in *R. eutropha*, mediates H<sub>2</sub> oxidation even in the presence of O<sub>2</sub>, thus providing an ideal model system for biological hydrogen production and utilization. The SH reversibly couples H<sub>2</sub> oxidation with the reduction of NAD<sup>+</sup> to NADH, thereby enabling the sustainable regeneration of this biotechnologically important nicotinamide cofactor. Thus, understanding the interaction of the SH with the cellular NADH/NAD<sup>+</sup> pool is of high interest. Here, we applied the fluorescent biosensor Frex to measure changes in cytoplasmic [NADH] in *R. eutropha* cells under different gas supply conditions. The results show that Frex is well-suited to distinguish SH-mediated changes in the cytoplasmic redox status from effects of general anaerobiosis of the respiratory chain. Upon H<sub>2</sub> supply, the Frex reporter reveals a robust fluorescence response and allows for monitoring rapid changes in cellular [NADH]. Compared to the Peredox fluorescence reporter, Frex displays a diminished NADH affinity, which prevents the saturation of the sensor under typical bacterial [NADH] levels. Thus, Frex is a valuable reporter for on-line monitoring of the [NADH]/[NAD<sup>+</sup>] redox state in living cells of *R. eutropha* and other proteobacteria. Based on these results, strategies for a rational optimization of fluorescent NADH sensors are discussed.

## Introduction

*Ralstonia eutropha* is a gram-negative  $\beta$ -proteobacterium endowed with a versatile and adaptive metabolism. The bacterium is able to oxidize organic compounds, preferably organic acids (heterotrophic growth), but is also capable of exploiting CO<sub>2</sub> and molecular hydrogen (H<sub>2</sub>) as carbon and energy sources (lithoautotrophic growth), respectively (Cramm, 2009). The ability to metabolize H<sub>2</sub> is mediated by four distinct [NiFe] hydrogenases in *R. eutropha* (Schäfer et al., 2013) that catalyze the (reversible) oxidation of molecular hydrogen in the presence of oxygen (O<sub>2</sub>) (Lenz et al., 2015). Two of these O<sub>2</sub>-tolerant hydrogenases are directly involved in energy conversion processes of the bacterium. The membrane-bound hydrogenase (MBH) oxidizes molecular hydrogen and channels the released electrons via a membrane-linked cytochrome *b* into the respiratory chain (Kalms et al., 2016). The second hydrogenase is the cytoplasmic soluble hydrogenase (SH), which couples H<sub>2</sub> oxidation to the reduction of oxidized nicotinamide adenine dinucleotide (NAD<sup>+</sup>) to NADH (Horch et al., 2012). NADH, can then be used as a reducing agent for, e.g., CO<sub>2</sub> fixation *via* the Calvin-Benson-Bassham cycle or for ATP generation *via* the respiratory chain (Cramm, 2009). Although biased towards H<sub>2</sub> oxidation, the SH is also capable of proton reduction and H<sub>2</sub> evolution under sufficiently reducing conditions in the cytoplasm (Kuhn et al., 1984). A crucial parameter to estimate the reduction potential of the cytoplasm is the [NADH]/[NAD<sup>+</sup>] ratio, as it (co-)defines the redox states of all the cellular NAD(H)-dependent enzymes and thus their catalytic activity (Lin and Guarente, 2003). Due to its high synthesis rate in living cells, both under aerobic and microaerobic conditions, the bidirectional SH activity affects the [NADH]/[NAD<sup>+</sup>] ratio significantly. It has therefore been postulated that a spectroscopic approach, which combines the measurement of intracellular [NADH]/[NAD<sup>+</sup>] levels with the functional state of the SH in living cells, would be highly beneficial for understanding the catalytic and physiological impact of this enzyme (Horch et al., 2015).

Many approaches have been utilized to measure the [NADH]/[NAD<sup>+</sup>] ratio as well as the individual concentrations of both nicotinamide derivatives in living cells, each with its own advantages and drawbacks. The simplest, yet utterly challenging, approach is to utilize the inherent fluorescence of NADH to estimate cellular concentrations (Rocheleau et al., 2004). However, this method does not allow estimating the ratio between the reduced and oxidized forms, since NAD<sup>+</sup> itself is not fluorescent. Furthermore, the fluorescence of NADH occurs in a spectral region that severely overlaps with cellular autofluorescence (Patterson et al., 2000). Also, the phosphorylated congener, NADPH, mostly involved in anabolic reactions, cannot be distinguished from NADH by standard fluorescence spectroscopy. Thus, the more demanding

method of fluorescence lifetime analysis is required to discriminate these molecular species (Blacker et al., 2014). However, a quantitative analysis by fluorescence lifetime imaging microscopy (FLIM) is difficult, because complex cellular samples usually show autofluorescence with multiexponential decay kinetics and ambiguous spectral shape.

Other approaches rely on lysis of cells and the investigation of [NADH]/[NAD<sup>+</sup>]-dependent redox couples, e.g., lactate and pyruvate, which are coupled to [NADH] and [NAD<sup>+</sup>] *via* the lactate dehydrogenase reaction (Bilan and Belusov, 2016; Williamson et al., 1967). However, since cells must be disrupted, on-line monitoring of nicotinamide cofactor levels in living cells is impossible with this method.

Recently, genetically engineered fluorescence sensors for the monitoring of [NADH] and [NADH]/[NAD<sup>+</sup>] in mammalian cell lines have been developed (Bilan et al., 2014; Hung et al., 2011; Zhao et al., 2011; Zhao and Yang, 2015). These sensors consist of bacterial NADH-binding proteins (so-called Rex repressor proteins) fused to a circularly permuted fluorescent protein (cpFP) (Baird et al., 1999), whose fluorescence response is highly sensitive towards structural changes. The Rex protein undergoes a significant conformational change upon NADH binding (Sickmier et al., 2005; Wang et al., 2008), which, in turn, modulates the fluorescence response of the cpFP.

Although derived from bacterial Rex repressor proteins, the [NADH] or [NADH]/[NAD<sup>+</sup>] sensors developed to date (Peredox (Hung et al., 2011), Frex/FrexH (Zhao et al., 2011) and SoNar (Zhao et al., 2015)) have been optimized for mammalian cell lines. Importantly, the total cellular NADH/NAD<sup>+</sup> pools and their ratio may differ substantially in mammalian and bacterial cells (Bennett et al., 2009; Zhao and Yang, 2012; Zhou et al., 2011). Indeed, the Peredox sensor (designed to report the [NADH]/[NAD<sup>+</sup>] ratio) was found to operate close to its saturation level when produced in *R. eutropha* cells grown under aerobic conditions, because its NADH sensitivity is in the lower nanomolar range (Tejwani et al., 2017; Zhao et al., 2011). Therefore, fluorescence sensors with diminished NADH affinity might be advantageous for their application in bacterial cells. Among the various genetically designed fluorescence probes, the Frex sensor has been constructed from the *Bacillus subtilis* Rex protein (genetically optimized to have a lower NADH sensitivity) and the circularly permuted yellow fluorescent protein, cpYFP (Zhao et al., 2011), serving as the chromophore. This sensor was initially established as a tool for determining absolute [NADH].

The goal of this work is to use the Frex sensor for sensing relative changes in NADH levels in *R. eutropha*, taking advantage of its lower NADH sensitivity compared to Peredox (Tejwani et al., 2017), but still bearing in mind the complex interaction of Frex with NADH and NAD<sup>+</sup>

based on our previous work (Wilkening et al., 2017). At  $\text{NAD}^+$  concentrations exceeding 100  $\mu\text{M}$ , the oxidized nicotinamide cofactor competes markedly with NADH for the binding site (Gyan et al., 2006) and, thereby, reduces the maximal fluorescence response of the Frex sensor in a concentration-dependent manner (Wilkening et al., 2017). However, since the cellular  $[\text{NAD}^+]$  is about two orders of magnitude larger than  $[\text{NADH}]$  (Bennett et al., 2009; Zhao and Yang, 2012), even large relative changes in  $[\text{NADH}]$  would typically be translated into small absolute changes in  $[\text{NAD}^+]$ . Consequently, any variation of the Frex fluorescence amplitude should predominantly report just  $[\text{NADH}]$  changes, while the corresponding  $[\text{NAD}^+]$  variations affect the sensor response only moderately. Indeed, our data show that upon Frex synthesis in *R. eutropha*, its fluorescence signal dynamically reflects changes of cellular  $[\text{NADH}]$  during the shift from aerobic to anaerobic conditions and in response to the availability of  $\text{H}_2$ , which can be unequivocally assigned to the activity of the SH.

## Materials and Methods

***Cloning of Frex gene into the pLO13-SH vector.*** The cDNAs coding for Frex and cpYFP (kind gift from Dr. William Oldham and Prof. Joseph Loscalzo, Harvard Medical School) were cloned into the pLO13-SH vector between the restriction sites of *NcoI* and *HindIII*. The *NcoI* restriction site was introduced by site-directed mutagenesis *via* recombinant PCR. PCR amplification primers were:

Forward Primer Frex: 5'-CGATAAGGAGCCCATGGATAAGG-3'

Forward Primer cpYFP: 5'-GGCTACCATGGCGGATCCG-3'

Reverse Primer: 5'-GCTAGTTATTGCTCAGCGG-3'

The pLO13-SH vector carries a tetracycline resistance gene, and transcription of the subcloned cDNA is under the control of the endogenous promoter for the soluble hydrogenase (SH).

***Conjugation of Frex and cpYFP pLO13-SH into the desired R. eutropha strains.*** *E. coli* S17-1 cells were transformed with the pLO13-SH plasmid vector carrying the cDNA of the fluorescent sensor protein and grown overnight in 10 mL of LB medium containing 10  $\mu\text{g/mL}$  tetracycline. Recipient *R. eutropha* strains HF798 ( $\text{SH}^+$ ,  $\text{MBH}^-$ , regulatory hydrogenase $^-$  ( $\text{RH}^-$ )) and HF500 ( $\text{SH}^-$ ,  $\text{MBH}^-$ ,  $\text{RH}^-$ ) (Horch et al., 2010; Kleihues et al., 2000) were also cultivated overnight in 10 mL LB medium. Cells were harvested and washed with 5 mL of

sterile H16 buffer (24 mM Na<sub>2</sub>HPO<sub>4</sub>·7H<sub>2</sub>O, 11 mM KH<sub>2</sub>PO<sub>4</sub>) and resuspended in 1 mL of H16 buffer. 200 µL of donor and recipient strains were given onto a LB agar plate and mixed by spot mating. After 6 h of incubation at 37 °C, the cells were scraped off the plate with a sterile glass pipette, washed in 5 mL of sterile H16 buffer, and resuspended in 1 mL of sterile H16 buffer. 100 µL of 10<sup>-4</sup>-fold diluted samples were streaked onto an FN (composition see below) agar plate containing 10 µg/mL tetracycline and grown for 3 days at 37 °C. Transconjugant colonies appeared and incorporation of the desired plasmid was checked by alkaline lysis (pH 12) of cells expressing Frex.

**Growth of *R. eutropha*.** *R. eutropha* cells were grown in FN medium (24 mM Na<sub>2</sub>HPO<sub>4</sub>·7H<sub>2</sub>O, 11 mM KH<sub>2</sub>PO<sub>4</sub>, 37 mM NH<sub>4</sub>Cl, 0.81 mM MgSO<sub>4</sub>·7H<sub>2</sub>O, 68 µM CaCl<sub>2</sub>·2H<sub>2</sub>O, 11 µM FeCl<sub>3</sub>·6H<sub>2</sub>O, 1 µM NiCl<sub>2</sub>, 0.4 % fructose, pH 7.3) or FGN medium (FN medium with 0.2 % fructose and 0.2 % glycerol) at 30 °C. Cells were grown to an OD<sub>600</sub> of 7 in the presence of 10 µg/mL tetracycline. Before fluorescence measurements of cells, tetracycline had to be removed from the medium, since the emission spectra of tetracycline and the Frex sensor overlap. Thus, cells were harvested and resuspended to a final OD<sub>600</sub> of 0.5 in fresh tetracycline-free GN medium (24 mM Na<sub>2</sub>HPO<sub>4</sub>·7H<sub>2</sub>O, 11 mM KH<sub>2</sub>PO<sub>4</sub>, 37 mM NH<sub>4</sub>Cl, 0.81 mM MgSO<sub>4</sub>·7H<sub>2</sub>O, 68 µM CaCl<sub>2</sub>·2H<sub>2</sub>O, 11 µM FeCl<sub>3</sub>·6H<sub>2</sub>O, 1 µM NiCl<sub>2</sub>, 0.4 % glycerol, pH 7.3).

**Alkaline Lysis.** *R. eutropha* cells were grown heterotrophically, harvested, and resuspended to a final OD<sub>600</sub> of 0.5 in H16 buffer (24 mM Na<sub>2</sub>HPO<sub>4</sub>·7H<sub>2</sub>O, 11 mM KH<sub>2</sub>PO<sub>4</sub>) at pH 11. Cells were incubated for 15 minutes, leading to lysis of the cells due to the alkaline environment. Suspensions of disrupted cells were subsequently examined by fluorescence spectroscopy.

**Gas incubation.** 1 mL aliquots of cell suspensions with a final OD<sub>600</sub> of 0.5 were bubbled for various time periods in a 2 mL quartz cuvette sealed with a rubber septum at a gas flow rate of 0.1 L/min at room temperature. Spectra were recorded immediately afterwards.

**Gas mixtures.** Cell suspensions with a final OD<sub>600</sub> of 0.5 were added to a mixture of aerated GN medium and H<sub>2</sub>-saturated GN medium in appropriate volume combinations to obtain the desired H<sub>2</sub> percentages. Cuvettes for fluorescence measurements were completely filled by the fluid phase.

**Fluorescence measurements.** Fluorescence was measured with a Fluoromax-2 spectrofluorometer (Horiba Jobin Yvon, Bensheim, Germany). Slits were set to 4 nm for excitation and 2 nm for emission, while the integration time was 1 s and the increment 1 nm. Frex was excited at 480 nm, and emission spectra were recorded in a suitable range centred around the emission maximum of 515 nm for evaluation of the amplitudes. cpYFP was excited at 480 nm for comparability of the fluorescence response with the derived sensors.

The titration data of the acquired fluorescence intensity  $F$  of Frex in lysed cells were analyzed by means of the Hill equation,

$$F = \frac{F_{\max} \cdot [\text{NADH}]^n}{K_D^n + [\text{NADH}]^n} \quad (\text{Eq. 1})$$

in which  $F_{\max}$  is the fluorescence in the presence of fluorescence-saturating NADH concentrations,  $K_D$  is the microscopic dissociation constant, and  $n$  is the cooperativity parameter.

Another approach to determine the dissociation constant  $K_D$  for the situation in lysed cells uses a quadratic formula to fit the titration data. In contrast to a classical hyperbolic curve (such as the Hill function in Eq. 1), the underlying model is free from assumptions regarding the concentrations of total and free titrant (receptor) and the binding stoichiometry (Swillens, 1995; Hulme and Trevithick, 2001).

$$\frac{[RL]}{[R_{\text{tot}}]} = \frac{[L_{\text{tot}}] + [R_{\text{tot}}] + K_D}{2 \cdot [R_{\text{tot}}]} - \sqrt{\left(\frac{[L_{\text{tot}}] + [R_{\text{tot}}] + K_D}{2 \cdot [R_{\text{tot}}]}\right)^2 - \frac{[L_{\text{tot}}]}{[R_{\text{tot}}]}} \quad (\text{Eq. 2})$$

In this formula,  $[RL]$  is the concentration of the Frex sensor protein with NADH bound (here reflected by the normalized fluorescence amplitude),  $[R_{\text{tot}}]$  is the total concentration of equivalent receptor binding sites (in  $\mu\text{M}$ ),  $[L_{\text{tot}}]$  is the total concentration of NADH present (“ligand”), and  $K_D$  represents the dissociation constant. Fitting the data using this equation yields two fit parameters,  $[R_{\text{tot}}]$  and  $K_D$ . If the binding stoichiometry  $n$  is known, the total receptor concentration can be calculated from the ratio  $[R_{\text{tot}}]/n$ .

Data processing was carried out using Origin 2017 software (OriginLab Corp., Northampton, MA, U.S.A.).

## Results

The cDNA for the Frex sensor was subcloned into the pLO13-SH vector, as described in materials and methods and previously (Tejwani et al., 2017). The resulting plasmid was introduced into the SH-expressing and SH-deficient *R. eutropha* strains HF798 (SH<sup>+</sup>, MBH<sup>-</sup>, RH<sup>-</sup>) and HF500 (SH<sup>-</sup>, MBH<sup>-</sup>, RH<sup>-</sup>), respectively (Horch et al., 2010; Kleihues et al., 2000). Since the fluorescence of the cpYFP moiety of the sensor increases strongly at alkaline pH (Schwarzländer et al., 2014), expression and functionality of the Frex sensor was confirmed *via* alkaline lysis of cells and subsequent measurement of the Frex fluorescence signal upon this alkaline treatment (Supplementary Figure 1).

We first aimed at inferring changes in cytoplasmic [NADH] by monitoring the fluorescence of Frex to establish a relationship between Frex fluorescence and SH activity by comparing Frex fluorescence in SH-synthesizing and SH-deficient *R. eutropha* strains. Therefore, we sought to elevate Frex fluorescence by treating Frex-synthesizing cells with H<sub>2</sub>. To delimit the effect of the H<sub>2</sub>-driven NAD<sup>+</sup> reduction activity of the SH on the cellular NADH pool from the more general effects of anoxic conditions and concomitant overreduction of the cytoplasm, we carried out control experiments with helium (He) treatment.

In a first set of experiments, Frex-containing *R. eutropha* cultures were treated with H<sub>2</sub> gas in a septum-sealed quartz cuvette under constant stirring, until a steady-state fluorescence amplitude was reached (10 minutes). This treatment led to a strong increase in the Frex fluorescence signal by about the same factor for the cells of both *R. eutropha* HF798 and HF500 (Fig. 1A,B).

The robust increase of the Frex signal upon H<sub>2</sub> treatment (Fig. 1A,B) indicates an increase in cytosolic [NADH]. This is in line with the expectation that treatment of *R. eutropha* cells with H<sub>2</sub> removed all O<sub>2</sub> from the samples. Since O<sub>2</sub> serves as the terminal electron acceptor of the respiratory chain (Cramm, 2009), its absence prevents NADH from being re-oxidized by Respiratory complex 1 (NADH:ubiquinone oxidoreductase), and NADH should accumulate in the cytoplasm. Notably, upon H<sub>2</sub> treatment, the fluorescence of the Frex sensor increases more than eightfold in both strains (Fig. 1A,B) indicating that the removal of O<sub>2</sub> and the concomitant blockage of the respiratory chain is mainly responsible for the acute rise in [NADH], irrespective of the presence or absence of the SH. Based on our previous study on the purified Frex protein, an eightfold increase of the Frex fluorescence corresponds to the

maximal extent of sensor signal augmentation at neutral pH. This dynamic range can only be achieved if the sensor response is saturated by NADH, and the free NAD<sup>+</sup> concentration in the cells is below 100 μM; otherwise NAD<sup>+</sup> would limit the maximal Frex response to NADH, as shown previously (Wilkening et al., 2017).

To test the hypothesis that O<sub>2</sub> removal is the main factor determining the acutely elevated [NADH] levels independent from the presence of SH, anoxic conditions were also induced by treatment with He gas (Fig. 1A,B). Upon He treatment, an elevated Frex signal of comparable relative amplitude was again observed in both (SH-expressing and SH-deficient) strains, and a rather fast signal decrease to the initial level occurred upon re-aeration (Fig. 1D,F) similar to the time course of the Frex signal observed for SH-deficient HF500 cells upon H<sub>2</sub>-treatment (Fig. 1E). The Frex signal increase caused by He treatment reached only 50 % of that of H<sub>2</sub>-treated cells. This behaviour might demand further elucidation, but since the same result was obtained for both *R. eutropha* strains (Fig. 1A,B), it is obviously not related to the presence or absence of SH activity. The observed differences might rather hint at the influence of the different physico-chemical properties of the two gases on the complex cellular response that eventually governs the NADH/NAD<sup>+</sup> levels in an anoxic response. For example, different Henry constants (Sander, 2015), diffusion constants (Engineering ToolBox, 2008) or water/lipid partition coefficients would all influence the availability of a particular gas in cells.

Remarkably, we found no significant difference regarding the H<sub>2</sub>-mediated *relative* increase of Frex fluorescence intensity in both strains (note that the overall fluorescence amplitudes in these experiments is dependent on cell density and expression level of the sensor). Thus, the immediate increase of the sensor fluorescence alone does not allow for discriminating effects on cellular [NADH] related to the presence of SH. However, the time courses of the decline of the fluorescence signals during re-aeration of the H<sub>2</sub> exposed cells were strikingly different for the two strains. In SH-deficient cells (HF500), the signal decreased to the initial basal value after about two minutes of aeration (Fig. 1E). In contrast, for the SH-expressing cells of the HF798 strain, the signal stayed elevated for about 30 minutes after re-exposure to atmospheric O<sub>2</sub>, and only after this period, the signal dropped sharply over the course of about one minute to the initial value (Fig. 1C). This indicates that in the presence of H<sub>2</sub>, continuous activity of SH leads to a steadily elevated [NADH] in strain HF798 (as long as H<sub>2</sub> is available, see below) but not in the SH-deficient strain HF500.

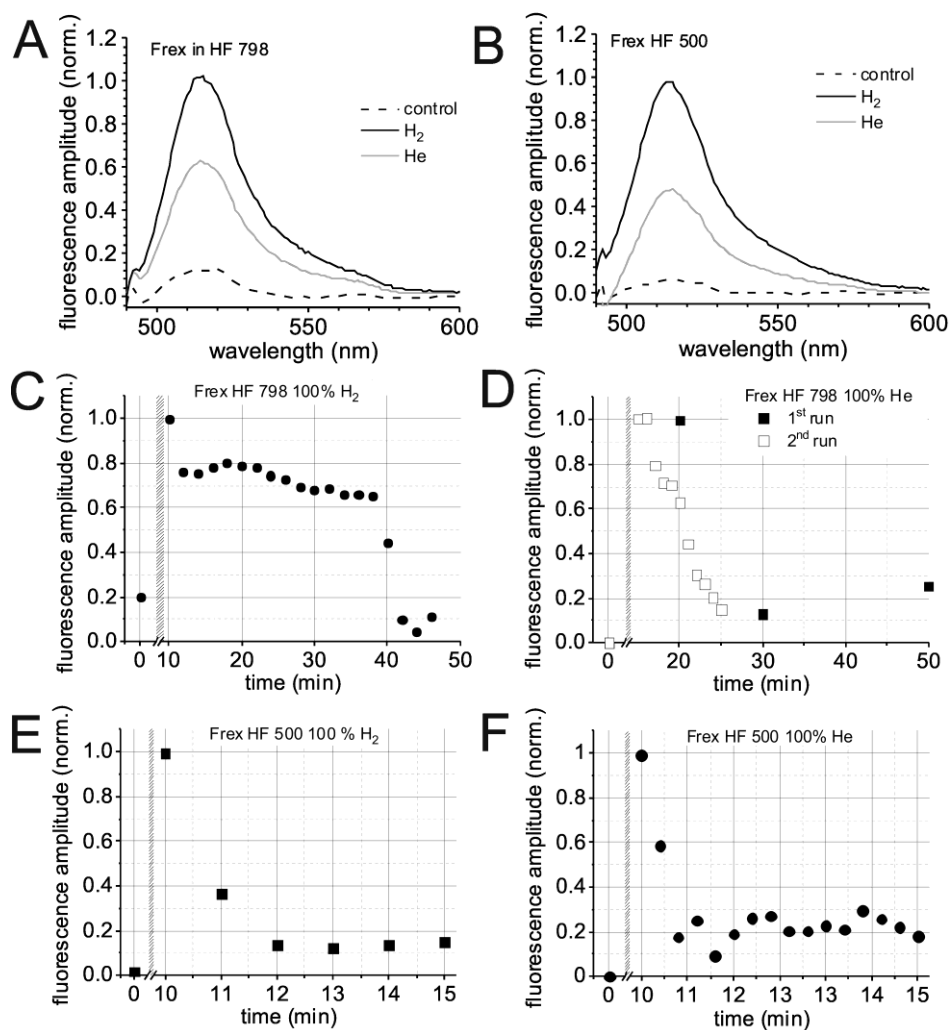


**Figure 1:** (A,B) Background-corrected and normalized fluorescence spectra of Frex-containing *R. eutropha* cell suspensions of the same OD<sub>600</sub> after excitation at 480 nm (see Supplementary Figure 2 for the background subtraction procedure). The relative increase in Frex fluorescence is higher for H<sub>2</sub> treatment than for helium treatment in both, the SH-expressing strain HF798 (A) and the SH-deficient strain HF500 (B), indicating that these immediate responses to anoxic conditions occur independent from the presence or absence of the SH. (C,D) Frex fluorescence response in the SH-expressing strain HF798 during and after treatment with H<sub>2</sub> (C) and helium (D). Panel (D) summarizes two experiments conducted on different time scales. (E,F) Frex fluorescence response in the SH-deficient strain HF500 during and after treatment with H<sub>2</sub> (E) and helium (F). Samples in (C-F) were treated in a sealed fluorescence cuvette with H<sub>2</sub> / He gas until the signal was stable, and then the septum was removed (axis break). Data points in (C-F) refer to background-corrected fluorescence levels at 515 nm (excited at 480 nm) normalized to values between 0 and 1, with 0 being the lowest fluorescence amplitude (at the Frex emission peak around 515 nm) and 1 the corresponding maximum amplitude measured immediately after removal of the septum.

At present, it is impossible to derive reliable quantitative information about NADH/NAD<sup>+</sup>

concentrations from the observed sensor responses, since the interaction of NADH and  $\text{NAD}^+$  with the Frex sensor is complex, as exemplified by the fact that the dynamic range of the sensor is limited, if  $\text{NAD}^+$  concentrations exceed  $100 \mu\text{M}$  (Wilkening et al., 2017). Thus, without further knowledge about the actual NAD(H) pool size, it is impossible to discriminate, whether the 50%-reduced response of the sensor in He- versus  $\text{H}_2$ -treated cells is, for example, due to a half-maximal NADH concentration ( $3.5 \mu\text{M}$ ) at zero  $[\text{NAD}^+]$  or due to the presence of  $100 \mu\text{M}$  NADH at about  $400 \mu\text{M}$   $\text{NAD}^+$  (see Fig. 1 and Fig. 2 in (Wilkening et al., 2017)). However, the very similar temporal Frex response pattern observed upon He treatment and subsequent re-aeration (Fig. 1D,F) shows that under anoxic conditions and recovery thereof, the cellular response is apparently independent from the presence of the SH. Upon limitation of the terminal electron acceptor  $\text{O}_2$ , NADH accumulates, but, as soon as  $\text{O}_2$  is available again, the fluorescence signal decreases on a relatively short time scale due to respiratory NADH consumption. In contrast, the constant high-level signal of the sensor, which only occurred in SH-expressing cells after  $\text{H}_2$  treatment (Fig. 1C) indicates sustained elevation of  $[\text{NADH}]$  due to the activity of the SH. The enzyme should be able to produce NADH as long as sufficient  $\text{H}_2$  concentrations are present in the cells during the recovery of atmospheric conditions (see below). This indicates that under the chosen experimental conditions, sufficient  $\text{H}_2$  is available for a certain time span (during re-exposure to air), before it is depleted from the solution by diffusion or consumption by the SH.

A caveat for using the Frex sensor in living cells is its pronounced pH-sensitivity, which is inherited from the cpYFP fluorophore (Day and Davidson, 2009; Schwarzländer et al., 2014; Zhao et al., 2011). cpYFP fluorescence can also be used to monitor possible intracellular pH changes. To delineate, whether cytoplasmic pH changes occur during the chosen experimental conditions, gas exchange experiments were carried out with *R. eutropha* cells synthesizing just the cpYFP fluorophore. When cpYFP-containing *R. eutropha* cells, cultivated under the same conditions as the Frex expressing cells used for the experiments shown in Figure 1, were subjected to the same  $\text{H}_2$  treatment as described in Figure 1 or to anaerobic conditions by flushing with He gas, the fluorescence amplitude did not change significantly (Supplementary Figure 3). Thus, substantial pH changes influencing the sensor's response can be excluded. Since the cpYFP fluorescence signal of intact cells was rather small, we needed to ascertain appropriate expression of cpYFP. For this purpose, the cells used for the experiments shown in Supplementary Figure 3 were subsequently lysed by resuspension in pH 11 buffer. After this treatment, strongly elevated fluorescence signals were observed, which demonstrates robust cpYFP synthesis in both *R. eutropha* strains. These control experiments support the

notion that the Frex signals observed under the conditions in living cells are not biased by concomitant pH changes in the cytoplasm.

Another set of experiments aimed at a differentiated response of the Frex sensor to different  $H_2/O_2$  ratios. For this purpose, pelleted cells were resuspended in different mixtures of a buffer equilibrated with the oxic atmosphere and another buffer saturated with  $H_2$ . By mixing these two buffers in different ratios and filling the cuvette completely, different  $H_2$  partial pressures could be realized while still having substantial  $O_2$  in the samples. These experiments revealed that the more  $H_2$  is available as SH substrate, which is metabolized to produce NADH, the longer the Frex fluorescence signal remains at an elevated level (Fig. 2A). The duration of elevated fluorescence shows a monotonous increase with increasing  $H_2$  partial pressure, whereas the maximal increase in fluorescence did not depend on this parameter (Fig. 2A). This supports the finding of Fig. 1C that the Frex fluorescence signal stays elevated until all  $H_2$  is consumed by SH (or diffused into the atmosphere) so that the NADH level drops significantly below the saturation level of the sensor.

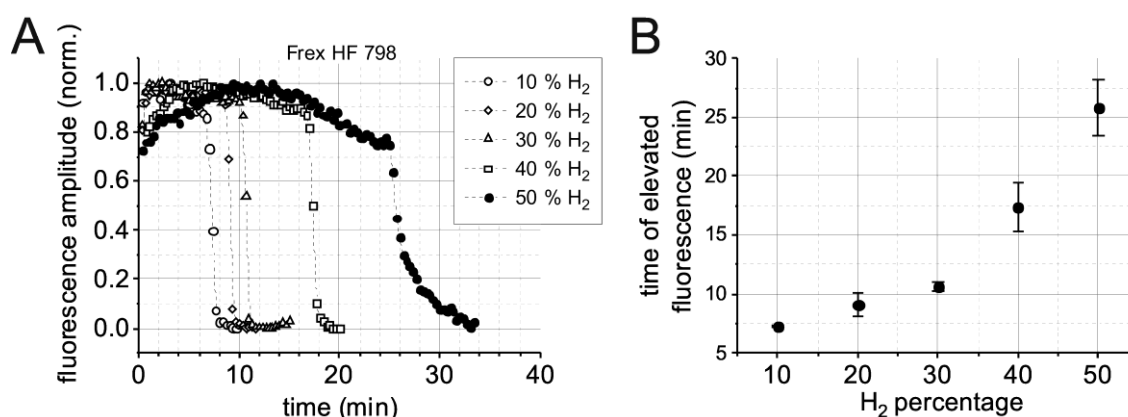


**Figure 2:** (A) Frex fluorescence in the presence of specified  $H_2$ /air mixtures ( $H_2$  content in % v/v as indicated) in the SH-expressing strain HF798. Excitation was carried out at 480 nm, and fluorescence emission maxima at 515 nm were plotted at various time points. Fluorescence signals were background-corrected and subsequently normalized to values between 0 and 1, with 0 being the lowest fluorescence amplitude (at the Frex emission peak around 515 nm) and 1 the corresponding maximum amplitude measured in the experiment. (B) Influence of the applied  $H_2$  percentage in the gas mixture (partial pressure) on the duration of elevated Frex fluorescence (time for signal decrease to 50% of the saturation value from experiments in panel (A)).

This indicates that even the lowest  $H_2$  concentration applied (10 % of partial pressure corresponds to about  $80 \mu M H_2$  as inferred from the Henry constant of  $H_2$  in aqueous solution, see (Sander, 2015)) was sufficient to allow the SH to produce [NADH] exceeding the saturation limit of the Frex sensor. Therefore, rather than the fluorescence intensity, which might be saturated over a wide range of  $H_2$  concentrations, the time duration of the elevated sensor fluorescence serves as a marker for the activity of the SH in living cells (Fig. 2B) in relation to availability of  $H_2$ .

Since the  $H_2$  concentration in the cell suspensions directly relates to the duration of elevated fluorescence, it should also be possible to alter the duration of elevated fluorescence not by changing substrate ( $H_2$ ) concentration, but by changing the amount of cells (i.e. the cell density) able to consume a given  $H_2$  concentration. This was verified by exposing HF798 cell suspensions of different optical densities to the same  $H_2$  partial pressure (Fig. 3).

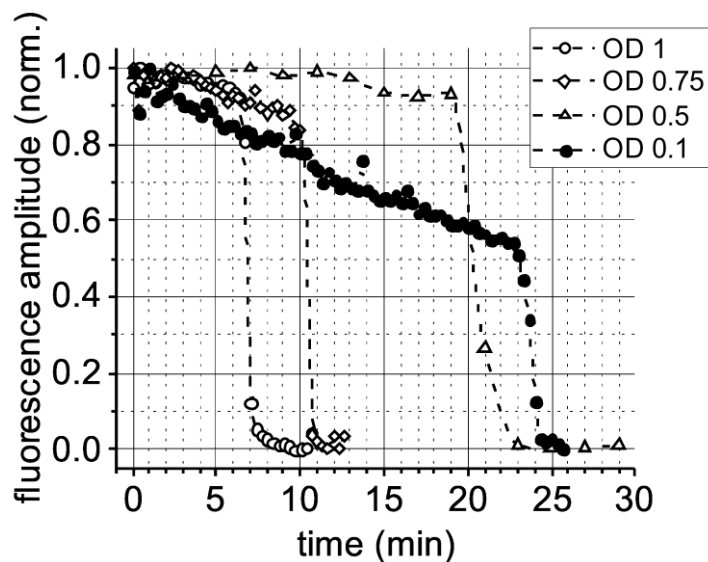


**Figure 3:** Frex fluorescence signals in the presence of 50 %  $H_2$  in *R. eutropha* HF798 cell suspensions of differing OD. Frex was excited at 480 nm and the fluorescence emission maxima at 515 nm were plotted at various times. The higher the total amount of SH in the samples (due to different cell densities indicated by the OD values), the faster the substrate  $H_2$  is metabolized. Fluorescence signals were background-corrected and subsequently normalized to values between 0 and 1, with 0 being the lowest fluorescence amplitude (at the Frex emission peak around 515 nm) and 1 the corresponding maximum amplitude measured in the experiment immediately after preparation of the samples.

To correlate the observed times of elevated (saturated) Frex sensor fluorescence in experiments on *R. eutropha* cell suspensions in buffers with different  $H_2$  partial pressures

(Fig. 2) or with different cell densities ( $OD_{600}$  values, Fig. 3) with the activity of the SH, we performed a hydrogenase activity assay. For this, *R. eutropha* cell suspensions were diluted to a certain OD in an  $H_2$ -saturated buffer containing 1 mM  $NAD^+$  and 0.005 % (w/v) of the surfactant cetyltrimethylammonium bromide (CTAB) to permeabilize the cells (see Supplementary Information). The metabolic activity of the hydrogenase was monitored by the increase of the NADH absorbance (extinction coefficient) at 365 nm over time. From these experiments, the NADH-producing activity of a cell lysate obtained from a suspension of cells of a certain OD could be determined. The  $H_2$  concentration of a 100 %  $H_2$ -saturated aqueous solution is about 800  $\mu$ M, as calculated from the corresponding Henry constant of  $H_2$  gas (Sander, 2015), and  $H_2$  concentrations at lower percentages can be determined, accordingly. With these  $[H_2]$  values and the metabolic activity stated above, one can calculate the “reaction times” ( $t_{calc}$ ), which *R. eutropha* cell suspensions of a given OD would need to metabolize a given  $[H_2]$ , in order to compare these with the experimentally observed times ( $t_{exp}$ ) of elevated Frex fluorescence from Figure 2B and Figure 3, as listed in Supplementary Tables 1 and 2. Of note, the calculated “reaction times” were in good agreement with the experimentally determined data, the only significant deviation occurred for the experiment with low cell density ( $OD_{600} = 0.1$ ).

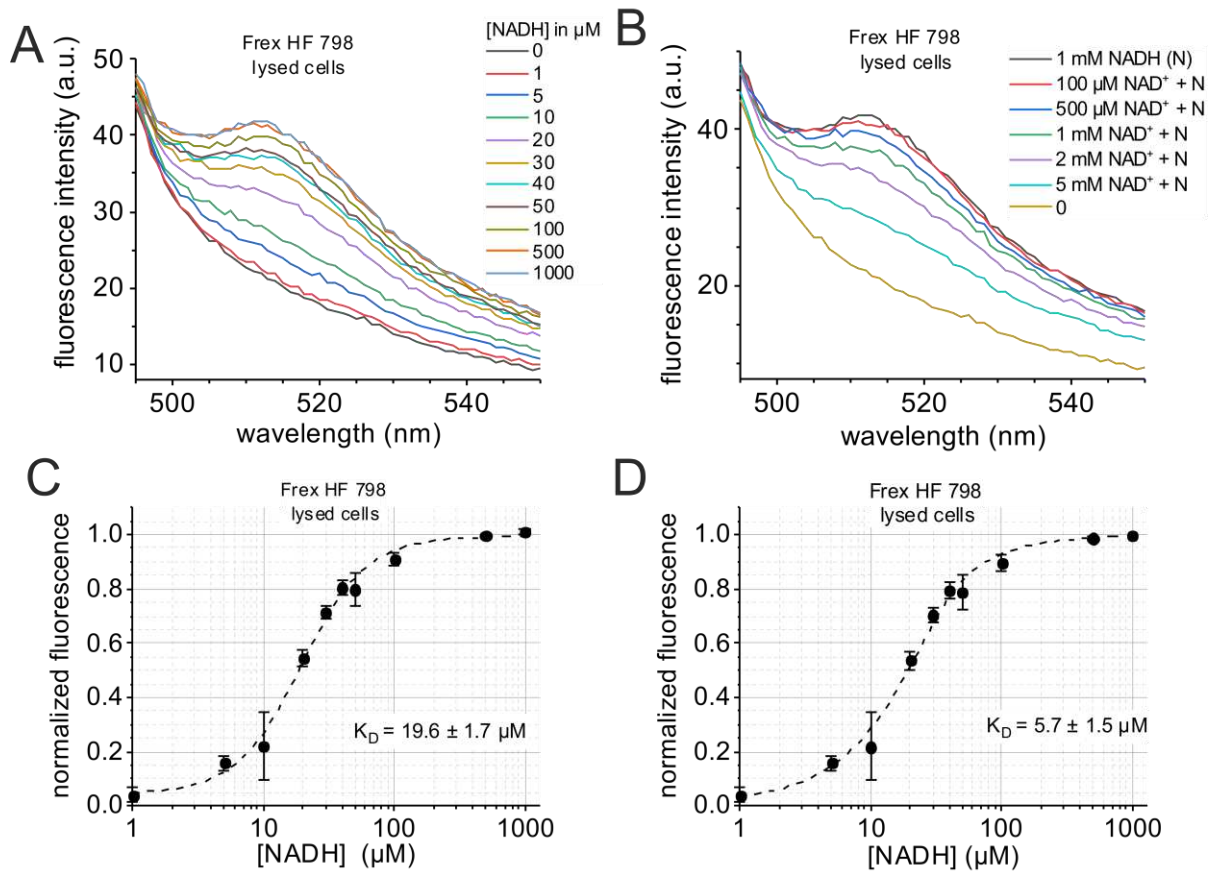
To reveal information about the intracellular concentrations of NADH and  $NAD^+$  in *R. eutropha*, we used a calibration technique as described previously for the fluorescence reporter Peredox in lysed cells (Tejwani et al., 2017). First, the Frex-expressing cells were sonicated, which led to a strong decrease of the fluorescence signal because of the dilution of the cellular constituents upon lysis. These lysates were subsequently used for NADH and  $NAD^+$  titration experiments while the corresponding fluorescence emission spectra were recorded (Figure 4).

Figure 4A shows the raw spectra obtained from the crude cell extract incubated with different amounts of NADH. The Frex sensor retained functionality after lysis and shows a dose-dependent response towards NADH. Compared to previous experiments on the purified sensor protein (Wilkening et al., 2017), in which an increase of the Frex fluorescence signal was already observed at 1  $\mu$ M NADH, somewhat higher NADH concentrations ( $[NADH] \geq 5$

$\mu\text{M}$ ) were required to enhance the sensor emission above the background signal. At  $[\text{NADH}]$  higher than  $500 \mu\text{M}$ , the fluorescence emission signal was saturated.

The concomitant  $\text{NAD}^+$  titration of the crude cell extract is shown in Figure 4B. First, a constant amount  $1 \text{ mM}$   $\text{NADH}$  was provided to robustly induce sensor emission. Subsequently, increasing  $\text{NAD}^+$  concentrations were added. This strategy was chosen because it has been previously shown that  $\text{NAD}^+$  reduces the emission of the Frex sensor by competing with  $\text{NADH}$  for the binding site(s) (Wilkening et al., 2017). Accordingly, we observed decreasing fluorescence signals with increasing  $[\text{NAD}^+]$ . As already mentioned for the  $\text{NADH}$  titration experiment, also for the  $\text{NAD}^+$  titration a somewhat larger concentration was needed to induce a significant signal decrease compared to the value determined with purified protein (Wilkening et al., 2017). Such deviations, which result in larger apparent  $K_D$  values determined from curve fitting, could arise if the concentration of the Frex sensor in the cell lysates would be in the same range as the  $K_D$  determined under well-defined conditions on the purified Frex protein (Hulme and Trevithick, 2010; Swillens, 1995). It also seems likely that the debris of cell constituents or membranes non-specifically scavenges  $\text{NAD(H)}$  to reduce the free  $\text{NAD(H)}$  concentration.

For quantitative data analysis, the spectra were background-corrected by subtracting the first spectrum after lysis (recorded at zero  $[\text{NADH}]$  or  $[\text{NAD}^+]$ ) from the subsequently recorded titration spectra. The spectra recorded in the absence of exogenously added nicotinamide cofactors do not show a significant contribution of Frex-specific emission and resemble the scattering background of the turbid lysates. Peak intensities of the background-corrected spectra at  $515 \text{ nm}$  were then normalized to values between 0 and 1, plotted against the  $\text{NADH}$  concentration (Fig. 4C), and fitted by a Hill function (Eq. 1) with the parameters shown in the inset. The calculated  $K_D$  value (microscopic dissociation constant) was  $(19.6 \pm 1.7) \mu\text{M}$  (with a Hill coefficient  $1.7 \pm 0.2$ ), which is larger than the  $K_D$  value of  $3.5 \mu\text{M}$  determined previously for the purified Frex protein (Wilkening et al., 2017). For a better analysis, we used a quadratic formula (Eq. 2) for fitting the data, which is derived from a reaction model that is free from assumptions regarding the concentrations of total and free titrant (receptor) as well as the binding stoichiometry (Hulme and Trevithick, 2010; Swillens, 1995). This model function compensates for the unknown receptor/sensor concentration, while determining the real dissociation constant. The  $K_D$  value derived from this fit (Fig. 4D) is about  $(5.7 \pm 1.5) \mu\text{M}$ , which is in better agreement with the determined  $K_D$  from measurements using the purified sensor protein ( $K_D = 3.5 \mu\text{M}$ , (Wilkening et al., 2017)).



**Figure 4:** Calibration for the Frex sensor response to NADH and NAD<sup>+</sup> in lysates of Frex-expressing cells with an OD of 0.1. (A,B) Unprocessed fluorescence emission spectra recorded in *R. eutropha* HF798 cell lysates upon excitation of Frex with 480 nm in the presence of various NADH concentrations (A) or different NAD<sup>+</sup> concentrations at a fixed [NADH] of 1 mM (B). Fluorescence signals were background-corrected and subsequently normalized to values between 0 and 1, with 0 being the lowest fluorescence amplitude (at the Frex emission peak around 515 nm) and 1 the corresponding maximum amplitude measured in the experiment. (C) Fits of the background-corrected and normalized fluorescence amplitudes from experiments as described in (A) with a Hill function. The resulting fit parameters are given in the inset (data from three experiments). (D) Fit of the data from (C) with a quadratic formula (eq. 2). The inset shows the resulting fit parameters (data from three experiments).

## Discussion

In order to determine differences in cytoplasmic NADH levels related to the activity of the soluble hydrogenase (SH), the fluorescence sensor Frex was stably expressed in different *R. eutropha* strains either containing (strain HF798) or devoid of the SH (strain HF500). The

monitoring of dynamic changes in [NADH] is of paramount importance to infer the metabolic status (redox state) of the cells. In theory, the different NADH levels in both cell strains should be attributable to the presence or absence of SH activity, especially if H<sub>2</sub> as substrate for the SH is available. However, control experiments are required to distinguish changes in [NADH] which are related to the activity of the SH from general effects of anaerobic conditions on the respiratory chain.

In measurements with H<sub>2</sub>-saturated cell suspensions of strain HF798 (SH<sup>+</sup>), a strong elevation of Frex sensor fluorescence was observed that reached a constant maximum level, which stayed constant for substantial time periods after re-aeration of the cell suspensions, and then dropped sharply to its basal value (Fig. 1C). In comparison, cells devoid of the SH showed a different time pattern of Frex sensor fluorescence. After a short fluorescence emission peak, the signal decreased upon re-oxygenation of the samples rather rapidly within about five minutes or less (Fig. 1E), a pattern that was also observed in both strains, if He treatment was used to induce anoxic conditions. Altogether, this indicates that the expressed SH in strain HF798 metabolized the supplied H<sub>2</sub> to yield NADH as long as sufficient H<sub>2</sub> is available in the system (Schneider and Schlegel, 1976). This activity of the SH keeps the [NADH]/[NAD<sup>+</sup>] ratio sufficiently high in order to stimulate Frex fluorescence over a prolonged period of time. Therefore, the Frex sensor is a convenient tool to monitor SH activity in living cells. Remarkably, initial elevation of the Frex fluorescence signal is apparently independent from the applied H<sub>2</sub> partial pressure, while the duration of the elevated fluorescence under re-aeration is correlated with the previously applied H<sub>2</sub> partial pressure (Fig. 2A) or the cell density (Fig. 3). These findings indicate (i) that the response of the Frex sensor is rapidly driven into saturation during gas treatment due to SH-dependent NADH production – even at low H<sub>2</sub> partial pressures – and (ii) that the duration of the elevated fluorescence signal is indicative of the amount of SH and its substrate (H<sub>2</sub>) present during the experiment (Fig. 2B and Fig. 3).

Thus, using the strategies established herein, the Frex [NADH] sensor is capable of determining SH activity in living cells in a variety of settings, since it shows a robust fluorescence response with a large dynamic range, which is dependent on the cellular NADH level. In contrast, the similar Peredox reporter protein with its NADH affinity in the low nanomolar range and its limited dynamic range (Hung et al., 2011; Zhao et al., 2011), showed only minute fluorescence increases under the same experimental conditions (Tejwani et al., 2017). Therefore, the about 100-fold lower NADH affinity of Frex provides a more valuable

tool for NADH detection in cellular settings under which NADH concentrations in the range of hundreds of micromolar are common, as in bacteria, with *R. eutropha* as a biotechnologically relevant example. However, the NADH levels in *R. eutropha* cells, especially under conditions of high SH activity, apparently also exceed the  $K_D$  value of the Frex sensor by far, so that the sensor cannot report the full range of cellular NADH concentrations. To adapt to this, further tailoring of the NADH affinity of the Frex sensor would be required. Nonetheless, although the Frex fluorescence response does not differ largely in intensity when exposed to different  $H_2$  partial pressures, it reports variant NADH levels in terms of the time period of the elevated fluorescence signal.

Even though the qualitative response of Frex can be unequivocally assigned to SH activity, it is not possible to quantitatively determine cellular NADH levels due to the antipodal effects of [NADH] and [NAD<sup>+</sup>] on the sensor response (Wilkening et al., 2017). While it was initially reported that the Frex sensor does not interact or alter fluorescence upon binding of the oxidized congener NAD<sup>+</sup> up to concentrations of 100  $\mu$ M (Zhao et al., 2011; Zhao and Yang, 2012), we found later that NAD<sup>+</sup> concentrations surpassing this value reduce the NADH-dependent fluorescence signal of Frex (Wilkening et al., 2017), in line with the NADH/NAD<sup>+</sup> dependence of the parental Rex protein reported previously (Gyan et al., 2006; Larsson et al., 2005; McLaughlin et al., 2010). In living *Ralstonia eutropha* cells, Frex shows its full dynamic range (determined for the purified sensor protein upon excitation at 480 nm (Wilkening et al., 2017)) under conditions of sufficient  $H_2$  supply. This indicates that the NAD<sup>+</sup> concentration is lowered to below 100  $\mu$ M by the activity of the SH, since larger NAD<sup>+</sup> concentrations would limit the dynamic range of the sensor (Wilkening et al., 2017). In our previous work, we estimated that the intracellular NAD<sup>+</sup> concentration in *R. eutropha* under aerobic conditions corresponds to 1.9 mM (Tejwani et al., 2017). On the one hand, one could infer from this that the maximal Frex fluorescence under aerobic conditions in *R. eutropha* must be affected by the basal NAD<sup>+</sup> levels and that quantitative NADH determination is not straightforward (Bennett et al., 2009; Tejwani et al., 2017; Zhou et al., 2011). On the other hand, the fact that  $H_2$  treatment (and anoxic conditions) induce(s) the maximum dynamic response of the sensor, at least indicates that the activity of the SH diminishes the free intracellular [NAD<sup>+</sup>] to (less than) 100  $\mu$ M with a concomitant increase in free [NADH] into the hundreds of  $\mu$ M range.

A drawback to the application of Frex in living cells is that only relative changes of its fluorescence amplitudes can be evaluated, while the dynamic range is influenced by several

factors including  $[\text{NAD}^+]$ . While our data show that Frex can be utilized to measure intracellular  $[\text{NADH}]$  changes in bacterial cells grown to the stationary phase, it would be of major interest to monitor the  $\text{NADH}/\text{NAD}^+$  redox state during the exponential growth phase. However, in a growing culture, the amount of Frex sensor per volume of cell suspension increases in a complicated manner dependent on cell density, and, concomitantly, the fluorescence signal increases in such a way that a correlation with the cellular  $[\text{NADH}]$  level is impossible. To resolve this, a signal normalization procedure would be necessary to allow for calibrating to the total amount of sensor protein in the sample, e.g. by utilization of an appropriate fluorescence standard, as in the Peredox sensor (Hung et al., 2011), which carries an additional red-emitting fluorophore for this purpose. In Frex, such an intrinsic normalization procedure would theoretically be possible by utilizing excitation within the other excitation band of the cpYFP chromophore (420 nm). However, the implementation of such a concept entails other experimental difficulties, since the fluorescence signal at 420 nm is much weaker and strongly overlaps with the cellular autofluorescence (Zhao et al., 2011). Thus, to avoid ambiguities due to the variable expression level of the sensor in cells, signal normalization could be facilitated by fusing a red fluorescent protein to Frex. Another point for improvement of the signal intensity would be to exchange the rather poor cpYFP fluorophore by a different one with a higher inherent brightness. Moreover, genetic engineering could be applied to develop sensor variants with further reduced  $[\text{NADH}]$  sensitivity, with eliminated  $\text{NAD}^+$  sensitivity, or with sensitivity to the  $[\text{NADH}]/[\text{NAD}^+]$  ratio.

Even though the Frex sensor has inherited a profound pH-sensitivity from its precursor cpYFP (Day and Davidson, 2009; Schwarzländer et al., 2014; Zhao et al., 2011), it could be ruled out that the sensor's response to  $\text{H}_2$  treatment of strain HF798 was significantly influenced by concomitant pH changes in the cytoplasm (Fig. 4). In line with previous observations for mammalian cells (Zhao et al., 2001), this observation indicates that cellular pH regulation in bacteria is under tight control even if large changes in the availability of metabolites are induced.

Despite certain limitations in quantitative studies, the robustness of the fluorescence signal makes the Frex sensor a promising candidate for biotechnological applications to monitor, optimize, or adjust bacterial culture conditions. Preliminary work on this approach is currently in progress and will be the subject of forthcoming studies. Future research might also utilize Frex to monitor SH activity and to correlate this information with insights from established

spectroscopic approaches such as IR or EPR spectroscopy in order to gather comprehensive information in living cells regarding the active states of NAD(H)-coupled hydrogenases, their reaction mechanism, and the parameters controlling their activity.

### **Acknowledgements**

The authors are grateful to Dr. William Oldham and Prof. Joseph Loscalzo (Harvard Medical School, USA) for providing the Frex expression clone. Work was funded by the Deutsche Forschungsgemeinschaft (DFG, German Research Foundation) under Germany's Excellence initiative 2005-2017 – EXC 314/1 (UniCat) and Germany's Excellence Strategy – EXC 2008/1 (UniSysCat) – 390540038.

## References

- Baird, G.S., Zacharias, D.A., and Tsien, R.Y. (1999). Circular permutation and receptor insertion within green fluorescent proteins. *Proceedings of the National Academy of Sciences of the United States of America*, 96(20), 11241–11246. <https://doi.org/10.1073/pnas.96.20.11241>
- Bennett, B., Kimball, E., and Gao, M. (2009). Absolute metabolite concentrations and implied enzyme active site occupancy in *Escherichia coli*. *Nature Chemical Biology*, 5(8), 593–599. <https://doi.org/10.1038/nchembio.186>
- Bilan, D.S. and Belousov, V.V. (2016). Genetically encoded probes for NAD<sup>+</sup>/NADH monitoring. *Free Radical Biology and Medicine*, 100(11), 32–42. <https://doi.org/10.1016/j.freeradbiomed.2016.06.018>
- Bilan, D.S., Matlashov, M.E., Gorokhovatsky, A.Y., Schultz, C., Enikolopov, G., and Belousov, V.V. (2014). Genetically encoded fluorescent indicator for imaging NAD<sup>+</sup>/NADH ratio changes in different cellular compartments. *Biochimica et Biophysica Acta - General Subjects*, 1840(3), 951–957. <https://doi.org/10.1016/j.bbagen.2013.11.018>
- Blacker, T.S., Mann, Z.F., Gale, J.E., Ziegler, M., Bain, A.J., Szabadkai, G., and Duchon, M.R. (2014). Separating NADH and NADPH fluorescence in live cells and tissues using FLIM. *Nature Communications*, 5(1), 3936. <https://doi.org/10.1038/ncomms4936>
- Cramm, R. (2009). Genomic View of Energy Metabolism in *Ralstonia eutropha* H16. *Journal of Molecular Microbiology and Biotechnology*, 16(1–2), 38–52. <https://doi.org/10.1159/000142893>
- Day, R.N. and Davidson, M.W. (2009). The fluorescent protein palette: Tools for cellular imaging. *Chemical Society Reviews*, 38(10), 2887–2921. <https://doi.org/10.1039/b901966a>
- Engineering ToolBox (2008). Diffusion coefficients of gases in water. [online] available at: [https://www.engineeringtoolbox.com/diffusion-coefficients-d\\_1404.html](https://www.engineeringtoolbox.com/diffusion-coefficients-d_1404.html) [accessed July 17,2019]
- Gyan, S., Shiohira, Y., Sato, I., Takeuchi, M., and Sato, T. (2006). Regulatory loop between redox sensing of the NADH/NAD<sup>+</sup> ratio by Rex (YdiH) and oxidation of NADH by NADH dehydrogenase Ndh in *Bacillus subtilis*. *Journal of Bacteriology*, 188(20), 7062–7071. <https://doi.org/10.1128/JB.00601-06>

- Horch, M., Hildebrandt, P., and Zebger, I. (2015). Concepts in bio-molecular spectroscopy : vibrational case studies on metalloenzymes. *Physical Chemistry Chemical Physics*, *17*, 18222–18237. <https://doi.org/10.1039/C5CP02447A>
- Horch, M. , Lauterbach, L. , Saggiu, M. , Hildebrandt, P. , Lenzian, F. , Bittl, R. , Lenz, O. and Zebger, I. (2010). Probing the Active Site of an O<sub>2</sub>-Tolerant NAD<sup>+</sup>-Reducing [NiFe]-Hydrogenase from *Ralstonia eutropha* H16 by In Situ EPR and FTIR Spectroscopy. *Angewandte Chemie International Edition*, *49*: 8026-8029. <https://doi.org/10.1002/anie.201002197>
- Horch, M., Lauterbach, L., Lenz, O., Hildebrandt, P., and Zebger, I. (2012). NAD(H)-coupled hydrogen cycling - Structure-function relationships of bidirectional [NiFe] hydrogenases. *FEBS Letters*, *586*(5), 545–556. <https://doi.org/10.1016/j.febslet.2011.10.010>
- Hulme, E.C. and Trevethick, M.A. (2010). Ligand binding assays at equilibrium: Validation and interpretation. *British Journal of Pharmacology*, *161*(6), 1219–1237. <https://doi.org/10.1111/j.1476-5381.2009.00604.x>
- Hung, Y.P., Albeck, J.G., Tantama, M., and Yellen, G. (2011). Imaging cytosolic NADH-NAD<sup>+</sup> redox state with a genetically encoded fluorescent biosensor. *Cell Metabolism*, *14*(4), 545–554. <https://doi.org/10.1016/j.cmet.2011.08.012>
- Kleihues, L., Lenz, O., Bernhard, M., Buhrke, T., and Friedrich, B. (2000). The H<sub>2</sub> sensor of *Ralstonia eutropha* is a member of the subclass of regulatory [NiFe] hydrogenases. *Journal of Bacteriology* *182*(10):2716–2724. <https://doi.org/10.1128/jb.182.10.2716-2724.2000>
- Kalms, J., Schmidt, A., Frielingsdorf, S., van der Linden, P., von Stetten, D., Lenz, O., Carpentier, P., and Scheerer, P. (2016). Krypton Derivatization of an O<sub>2</sub> -Tolerant Membrane-Bound [NiFe] Hydrogenase Reveals a Hydrophobic Tunnel Network for Gas Transport. *Angewandte Chemie International Edition Engl.* *55*(18):5586-90. <https://doi.org/10.1002/anie.201508976>
- Kuhn, M., Steinbüchel, A., and Schlegel, H.G. (1984). Hydrogen evolution by strictly aerobic hydrogen bacteria under anaerobic conditions. *Journal of Bacteriology*, *159*(2), 633–639.
- Larsson, J.T., Rogstam, A., and von Wachenfeldt, C. (2005). Coordinated patterns of cytochrome bd and lactate dehydrogenase expression in *Bacillus subtilis*. *Microbiology*, *151*(10), 3323–3335. <https://doi.org/10.1099/mic.0.28124-0>

- Lenz, O., Lauterbach, L., Frielingsdorf, S., and Friedrich, B. (2015). Oxygen-tolerant hydrogenases and their biotechnological potential. *Biohydrogen*, 61–96. <https://doi.org/10.1515/9783110336733.61>
- Lin, S. J. and Guarente, L. (2003). Nicotinamide adenine dinucleotide, a metabolic regulator of transcription, longevity and disease. *Current Opinion in Cell Biology*, 15(2), 241–246. [https://doi.org/10.1016/S0955-0674\(03\)00006-1](https://doi.org/10.1016/S0955-0674(03)00006-1)
- McLaughlin, K.J., Strain-Damerell, C.M., Xie, K., Brekasis, D., Soares, A.S., Paget, M.S.B., and Kielkopf, C.L. (2010). Structural basis for NADH/NAD<sup>+</sup> redox sensing by a Rex family repressor. *Molecular Cell*, 38(4), 563–575. <https://doi.org/10.1016/j.molcel.2010.05.006>
- Patterson, G.H., Knobel, S.M., Arkhammar, P., Thastrup, O., and Piston, D. W. (2000). Separation of the glucose-stimulated cytoplasmic and mitochondrial NAD(P)H responses in pancreatic islet beta cells. *Proceedings of the National Academy of Sciences of the United States of America*, 97(10), 5203–5207. <https://doi.org/10.1073/pnas.090098797>
- Rocheleau, J.V., Head, W.S., and Piston, D.W. (2004). Quantitative NAD(P)H/flavoprotein autofluorescence imaging reveals metabolic mechanisms of pancreatic islet pyruvate response. *Journal of Biological Chemistry*, 279(30), 31780–31787. <https://doi.org/10.1074/jbc.M314005200>
- Sander, R. (2015). Compilation of Henry's law constants (version 4.0) for water as solvent. *Atmospheric Chemistry and Physics* 15:4399-4981. <https://doi.org/10.5194/acp-15-4399-2015>
- Schäfer, C., Friedrich, B., and Lenz, O. (2013). Novel, oxygen-insensitive group 5 [NiFe]-hydrogenase in *Ralstonia eutropha*. *Applied and Environmental Microbiology*, 79(17), 5137–5145. <https://doi.org/10.1128/AEM.01576-13>
- Schneider, K. and Schlegel, H. G. (1976). Purification and properties of soluble hydrogenase from *Alcaligenes eutrophus* H 16. *Biochimica et Biophysica Acta (BBA) - Enzymology*, 452(1), 66–80. [https://doi.org/10.1016/0005-2744\(76\)90058-9](https://doi.org/10.1016/0005-2744(76)90058-9)
- Schwarzländer, M., Wagner, S., Ermakova, Y.G., Belousov, V.V., Radi, R., Beckman, J.S., Buettner, G.R., Demaurex, N., Duchen, M.R., Forman, H.J., Fricker, M.D., Gems, D., Halestrap, A.P., Halliwell, B., Jakob, U., Johnston, I.G., Jones, N.S., Logan, D.C., Morgan, B., Müller, F.L., Nicholls, D.G., Remington, S.J., Schumacker, P.T., Winterbourn, C.C., Sweetlove, L.J., Meyer, A.J., Dick, T.P., Murphy, M.P. (2014). The

- 'mitoflash' probe cpYFP does not respond to superoxide. *Nature*, 514(7523), E12–E14. <https://doi.org/10.1038/nature13858>
- Sickmier, E.A., Brekasis, D., Paranawithana, S., Bonanno, J.B., Paget, M.S.B., Burley, S.K., and Kielkopf, C.L. (2005). X-Ray structure of a Rex-family repressor/NADH complex insights into the mechanism of redox sensing. *Structure*, 13(1), 43–54. <https://doi.org/10.1016/j.str.2004.10.012>
- Swillens, S. (1995). Interpretation of binding curves obtained with high receptor concentrations: practical aid for computer analysis. *Molecular Pharmacology*, 47(6), 1197–1203.
- Tejwani, V., Schmitt, F.-J., Wilkening, S., Zebger, I., Horch, M., Lenz, O., and Friedrich, T. (2017). Investigation of the NADH/NAD<sup>+</sup> ratio in *Ralstonia eutropha* using the fluorescence reporter protein Peredox. *Biochimica et Biophysica Acta - Bioenergetics*, 1858(1), 86–94. <https://doi.org/10.1016/j.bbabi.2016.11.001>
- Wang, E., Bauer, M.C., Rogstam, A., Linse, S., Logan, D.T., and von Wachenfeldt, C. (2008). Structure and functional properties of the *Bacillus subtilis* transcriptional repressor Rex. *Molecular Microbiology*, 69(2), 466–478. <https://doi.org/10.1111/j.1365-2958.2008.06295.x>
- Wilkening, S., Schmitt, F.-J., Horch, M., Zebger, I., Lenz, O., and Friedrich, T. (2017). Characterization of Frex as an NADH sensor for *in vivo* applications in the presence of NAD<sup>+</sup> and at various pH values. *Photosynthesis Research*, 133(1–3), 305–315. <https://doi.org/10.1007/s11120-017-0348-0>
- Williamson, D., Lund, P., and Krebs, H. (1967). The redox state of free nicotinamide-adenine dinucleotide in the cytoplasm and mitochondria of rat liver. *Biochemical Journal*, 103(2), 514–527. <https://doi.org/10.1042/bj1030514>
- Zhao, Y., Hu, Q., Cheng, F., Su, N., Wang, A., Zou, Y., Hu, H., Chen, X., Zhou, H.M., Huang, X., Yang, K., Zhu, Q., Wang, X., Yi, J., Zhu, L., Qian, X., Chen, L., Tang, Y., Loscalzo, J., and Yang, Y. (2015). SoNar, a highly responsive NAD<sup>+</sup>/NADH sensor, allows high-throughput metabolic screening of anti-tumor agents. *Cell Metabolism*, 21(5), 777–789. <https://doi.org/10.1016/j.cmet.2015.04.009>
- Zhao, Y., Jin, J., Hu, Q., Zhou, H.-M., Yi, J., Yu, Z., Wang, X., Yang, Y., and Loscalzo, J. (2011). Genetically encoded fluorescent sensors for intracellular NADH detection. *Cell Metabolism*, 14(4), 555–66. <https://doi.org/10.1016/j.cmet.2011.09.004>

- Zhao, Y. and Yang, Y. (2012). Frex and FrexH: Indicators of metabolic states in living cells. *Bioengineered Bugs*, 3(3), 181–188. <https://doi.org/10.4161/bbug.19769>
- Zhao, Y. and Yang, Y. (2015). Profiling metabolic states with genetically encoded fluorescent biosensors for NADH. *Current Opinion in Biotechnology*, 31, 86–92. <https://doi.org/10.1016/j.copbio.2014.08.007>
- Zhou, Y., Wang, L., Yang, F., Lin, X., Zhang, S., and Zhao, Z.K. (2011). Determining the extremes of the cellular NAD(H) level by using an *Escherichia coli* NAD<sup>+</sup>-auxotrophic mutant. *Applied and Environmental Microbiology*, 77(17), 6133–6140. <https://doi.org/10.1128/AEM.00630-11>

## Supplementary Information to:

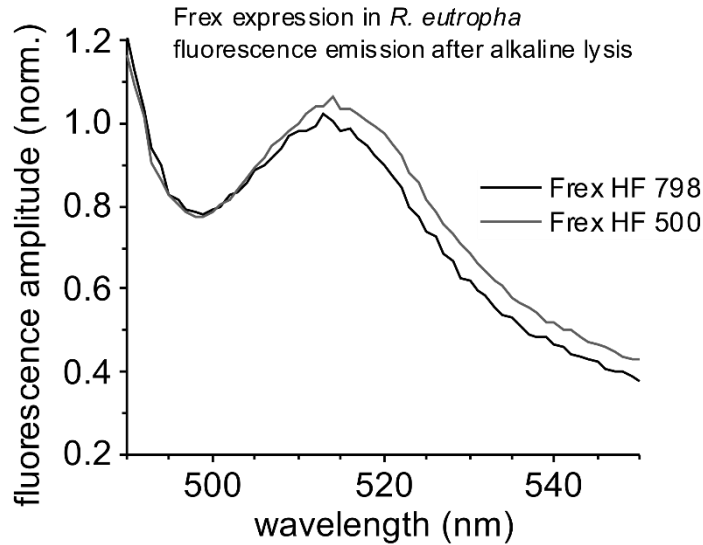
# Discriminating changes in intracellular NADH/NAD<sup>+</sup> levels due to anoxicity and H<sub>2</sub> supply in *R. eutropha* cells using the Frex fluorescence sensor

Authors: S. Wilkening<sup>1</sup>, F.-J. Schmitt<sup>1</sup>, O. Lenz<sup>1</sup>, I. Zebger<sup>1</sup>, M. Horch<sup>1,2</sup>, and T. Friedrich<sup>1\*</sup>

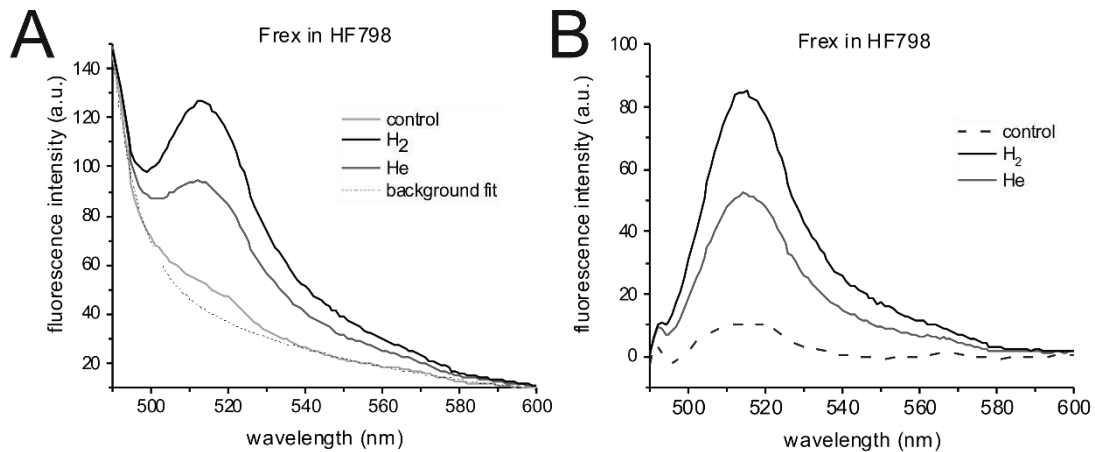
<sup>1</sup> Technische Universität Berlin, Institut für Chemie PC 14, Straße des 17. Juni 135, 10623 Berlin, Germany

<sup>2</sup> Department of Chemistry and York Biomedical Research Institute, University of York, YO10 5DD, United Kingdom

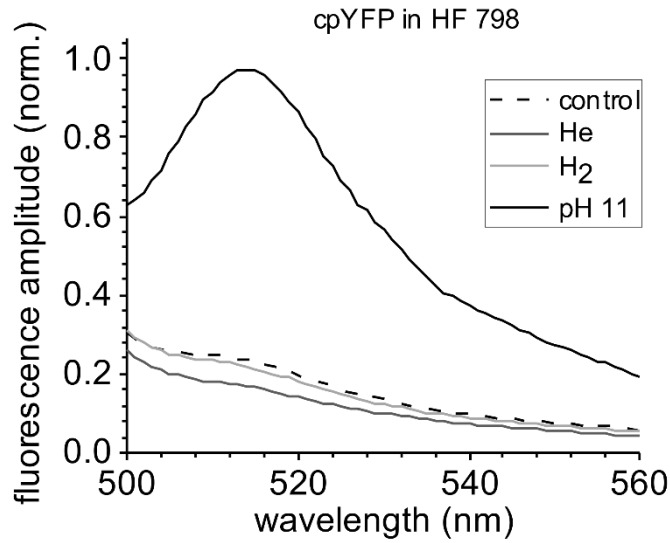
\* Corresponding author, E-mail: [friedrich@chem.tu-berlin.de](mailto:friedrich@chem.tu-berlin.de)



**Supplementary Figure 1:** Test for expression of Frex in *R. eutropha* strains upon alkaline cell lysis by treatment with pH 11 buffer. Frex fluorescence was excited at 480 nm, and spectra were normalized to the maximum of the Frex signal from the HF 798 strain at 512 nm for comparison.



**Supplementary Figure 2:** Procedure to subtract non-specific background from fluorescence signals of Frex-expressing *R. eutropha* cultures. Panel (A) shows raw fluorescence spectra of a cell suspension without and with gas treatment; high background due to light scattering by cells and their components is clearly visible. To compensate for this background, we calculated a biexponential curve (“background fit”, dotted line) by fitting the data of the “control” trace (representing the spectrum of the cell suspension before gas treatment) below 500 nm and above 540 nm with a biexponential function. Fitting by a biexponential curve yielded a better approximation than a typical  $\lambda^{-4}$  scattering function. Subtraction of the “background fit” curve obtained in this way from the raw spectra allows selecting the Frex fluorescence signal around 510 nm from the scattering background. Panel (B) shows the resulting background-subtracted spectra, which correspond to the curves shown in Figure 1A of the main text.



**Supplementary Figure 3:** Fluorescence spectra from *R. eutropha* cells (strain HF798) expressing cpYFP and lysates derived thereof after excitation at 480 nm. The fluorescence before (dashed line) and after alkaline lysis in buffer with pH 11 (black) as well as after treatment of intact cells with H<sub>2</sub> (light gray) or helium (gray) are shown.

## Correlation of elevated Frex fluorescence with hydrogenase activity

To compare the times of elevated (saturated) Frex sensor fluorescence observed in experiments on *R. eutropha* cell suspensions in buffers with different H<sub>2</sub> concentrations (Fig. 2) or with different cell densities (OD<sub>600</sub> values, Fig. 3) to the activity of the SH, we adapted a hydrogenase activity assay described by B. Friedrich and coworkers [1] for application to permeabilized *R. eutropha* cells. To this end, concentrated *R. eutropha* cell suspensions of a certain OD<sub>435</sub> were diluted in a H<sub>2</sub>-saturated buffer containing 1 mM NAD<sup>+</sup>, which was supplemented with the surfactant cetyltrimethylammonium bromide (CTAB) to permeabilize the cell membranes. The metabolic activity of hydrogenase in the presence of H<sub>2</sub> and NAD<sup>+</sup> was monitored as the increase of the NADH-specific absorbance at 365 nm based on an extinction coefficient of  $\epsilon_{365} = 3400 \text{ M}^{-1} \text{ cm}^{-1}$ .

In detail, 5  $\mu\text{L}$  of a concentrated cell suspension with an OD<sub>435</sub> of 118 were diluted in 2 mL H<sub>2</sub>-saturated, CTAB-containing buffer, resulting in an OD<sub>435</sub> of 0.295. The hydrogenase activity per OD<sub>435</sub> of the initial cell suspension can be calculated as follows:

$$A_{(\text{OD}_{435})} = \frac{\frac{\Delta\text{OD}_{365}}{\Delta t} \cdot V_t}{\epsilon_{365} \cdot d \cdot \text{OD}_{435}}$$

The increase of NADH extinction in time  $\frac{\Delta\text{OD}_{365}}{\Delta t}$  was calculated to  $0.016 \text{ min}^{-1}$ , the total volume  $V_t$  of the cell suspension was 2 mL in a cuvette with a path length ( $d$ ) of 1 cm, which results in

$$A_{(\text{OD}_{435}=1)} = \frac{0.016 \text{ min}^{-1} \cdot 0.002 \text{ L}}{3400 \text{ L mol}^{-1} \text{ cm}^{-1} \cdot 1 \text{ cm} \cdot 0.295} = 31.9 \text{ nmol min}^{-1}$$

Thus, under the crude assumption of constant enzyme activity, 2 mL of a *R. eutropha* cell suspension (lysate) of OD<sub>435</sub> = 1 would produce (consume) 31.9 nanomoles of NADH (H<sub>2</sub>) per minute. Since in *R. eutropha* cell suspensions of an OD<sub>435</sub> of 1 corresponds to an OD<sub>600</sub> of 0.5 (as applied in our experiments with different H<sub>2</sub> partial pressures), and we also used 2 mL samples of cell suspensions, the activity value of  $31.9 \text{ nmol min}^{-1}$  can be used to approximate the times needed to consume a certain H<sub>2</sub> concentration<sup>1</sup>.

We are aware of the fact that the assumption of a zero-order reaction (constant enzyme turnover) over the whole period of H<sub>2</sub> consumption by hydrogenases is a rough approximation, and that the calculated times for H<sub>2</sub> consumption represent only crude lower limits, since the concentration dependence of enzyme activity implies that the rate of H<sub>2</sub> consumption decreases over time. However, considering the complex reaction balance in the cell lysates used here, a precise model including all (partly unknown and probably counteracting) factors is currently out of reach. Moreover, reactions consuming (producing) NADH in the cell may also exert an influence on the duration of the Frex signal so that the

---

<sup>1</sup>From the values stated here, the hydrogenase activity per cell for a cell suspension of OD<sub>600</sub> = 0.5 (1 mL of a bacterial suspension with OD<sub>600</sub> of 1, or 2 mL with OD<sub>600</sub> of 0.5, correspond to about  $10^9$  cells) can be calculated as  $3.2 \cdot 10^5 \text{ s}^{-1}$ , which, together with the assumption of a hydrogenase turnover rate of about  $150 \text{ s}^{-1}$  [2], would result in an estimate of 2200 hydrogenase molecules per cell, which – in terms of the order of magnitude – matches well with the number of 400 to 2000 [NiFe]-hydrogenase molecules determined by ICP-MS in the similarly sized cyanobacterium *Synechocystis sp.* PCC 6803 [3].

time of elevated Frex fluorescence, during which the NADH concentration is saturating for Frex fluorescence, would represent a lower limit for NADH production by hydrogenases as well. Therefore, the *ad hoc* approach taken here represents a zero-order approximation that needs to be taken with caution.

The H<sub>2</sub> concentration of a saturated aqueous solution at standard ambient temperature and pressure (SATP) can be calculated using the corresponding Henry constant of H<sub>2</sub> gas ( $K_H=1282.05 \text{ L}\cdot\text{atm}\cdot\text{mol}^{-1}$ ), which results in a concentration of about 800  $\mu\text{M}$  H<sub>2</sub> gas at 100 % saturation. With this value and the metabolic activity stated above, one can approximately calculate the time  $t_{\text{calc}}$ , which a *R. eutropha* cell suspension of a given OD<sub>600</sub> and volume (here 2 mL) would need to metabolize a given [H<sub>2</sub>], as denoted in the following Supplementary Table 1 in comparison to the time of elevated Frex fluorescence ( $t_{\text{exp}}$ ) from Fig. 2B:

**Supplementary Table 1:**

Volume percent H <sub>2</sub>	n(H <sub>2</sub> ) in 2 mL (in nmol)	$t_{\text{calc}}$ (in min)	$t_{\text{exp}}$ (in min)
10	160	5.0	7.2
20	320	10.0	9.1
30	480	15.0	10.7
40	640	20.1	17.3
50	800	25.1	25.8 <sup>#</sup>

Similarly, the times needed to consume H<sub>2</sub> from a 50 % H<sub>2</sub>-saturated buffer by *R. eutropha* suspensions of different OD<sub>600</sub> (Fig. 3) can be calculated as listed in Supplementary Table 2, as compared to the observed times of elevated Frex fluorescence ( $t_{\text{exp}}$ ):

**Supplementary Table 2:**

OD <sub>600</sub>	Activity A (in nmol min <sup>-1</sup> )	$t_{\text{calc}}$ (in min)	$t_{\text{exp}}$ (in min)
1	63.8	12.5	6.9
0.75	47.9	16.7	10.4
0.5	31.9	25.1	20.9 <sup>#</sup>
0.1	6.4	125	23.7

The  $t_{\text{exp}}$  values marked with “#” in the Supplementary Tables 1 and 2 above were determined under identical conditions. The determined values vary by about 5 min providing an estimate of the experimental error. Considering this magnitude of the experimental error, the calculated reaction times correlate quite well with the theoretical reaction times, indicating that the

elevated Frex fluorescence signal serves as a measure of total hydrogenase activity in living *R. eutropha* cells. A substantial deviation is apparent for the very dilute sample with low cell density (OD<sub>600</sub> of 0.1) in Supplementary Table 2, in which the calculated reaction time is much larger than the observed reaction time. This deviation might be attributed to substantial effusion of H<sub>2</sub> from the solution (into the essentially H<sub>2</sub>-free atmosphere) considering a half-life time for H<sub>2</sub> in aqueous buffer of about 120 min (which would, of course, be modified by the geometry of the container, agitation, temperature etc.). Thus, the experimentally determined reaction times of up to 25 min are not seriously affected by H<sub>2</sub> effusion.

### **Literature cited:**

- [1] Friedrich, B., Heine, E., Fink, A., and Friedrich, C.B. (1981). Nickel Requirement for active hydrogenase formation in *R. eutropha*. *Journal of Bacteriology* **145**(3):1144-1149.
- [2] Ratzka, J., Lauterbach, L., Lenz, O., and Ansorge-Schumacher, M.B. (2011). Systematic evaluation of the dihydrogen-oxidising and NAD<sup>+</sup>-reducing soluble [NiFe]-hydrogenase from *Ralstonia eutropha* H16 as a cofactor regeneration catalyst. *Biocatalysis and Biotransformation* **29**:246-252, doi:10.3109/10242422.2011.615393
- [3] Gutekunst, K., Hoffmann, D., Westernströer, U., Schulz, R., Garbe-Schönberg, D., and Appel, J. (2018). In-vivo turnover frequency of the cyanobacterial NiFe-hydrogenase during photohydrogen production outperforms in-vitro systems. *Scientific Reports* **8**:6083, doi:10.1038/s41598-018-24430-y